Digest Journal of Nanomaterials and Biostructures Vol. 5, No 3, July-September 2010, p. 683-689

HYBRID SILICA-METALLOPORPHYRIN NANOMATERIALS EXHIBITING INTENSIVE ABSORPTION OF LIGHT IN THE RED-REGION

C. ENACHE[a], E. FAGADAR-COSMA[a*], I. ARMEANU[a], Z. DUDAS[a], C. IANASI[a], M. VASILE[b], D. DASCALU[c]
[a]*Institute of Chemistry Timisoara of Romanian Academy, M. Viteazul Ave, No. 24, 300223-Timisoara, Romania*
[b]*National Institute for Research and Development in Electrochemistry and Condensed Matter, P. Andronescu Street, No. 1, 300224- Timisoara, Romania.*
[c]*West University of Timisoara, Pestalozzi Street, No 16, 300115 - Timisoara, Romania.*

This work is focused on *in situ* entrapping of 5,10,15,20-Tetrakis(4-pyridyl)porphyrin-Zn(II), (ZnTPyP), by sol-gel technique, starting from tetraethylorthosilicate (TEOS). The sol-gel process was conducted by acid or acid-base catalysis, followed by sonication. Nanomaterials with high surface area (350-730 m^2/g), narrowly distributed pore size (2-3.8 nm), exhibiting intensive absorption of light in the red-region up to 700-800 nm have been obtained. A comparison between the properties of the obtained hybrids as a consequence of the used catalytic system and of supplementary treatments is done.

(Received July 15, 2010; accepted August 27, 2010)

Keywords: Metalloporphyrin, Silica hybrids, Sol-gel preparation, Luminescence, Nanomaterials

1. Introduction

Nowadays Zn-porphyrins receive great interest of scientists due to their amazing applications in physics (photovoltaic cells [1, 2]), chemistry (supramolecular chemistry [3, 4], biomimetic substances, chemical and electrochemical sensors for selective detection of various analytes [5-8], catalysts and photocatalysts in micro-channel chips [9]), material science (hybrid materials with special optoelectronic properties [10]) and medicine (photosensitizers in photodynamic therapy [11], treatment of malaria, antimicotic and antimicrobial agents [12]). The adsorption of Zn metalloporphyrins to mesoporous silica was investigated for construction of photosynthetic and chromatographic applications. Zn (II)-porphyrins are used as HPLC stationary phase for amino acids, peptides, and oligopeptides separations [13]. A major target of nanotechnology research is the formulation of functional nanoscale molecular devices based on supramolecular structures. The molecular self-assemblies of zinc meso-tetra(4-pyridyl)porphyrin (ZnTPyP) in the presence of a surfactant were reported to give hexagonal nanoprism with a large cavity of about 19 Å [14]. Recently, immobilisation of zinc porphyrin complexes on an inorganic support was done by using 'click' immobilisation techniques involving an azide linked to a high density silica support. The novel materials were tested as recycling catalysts in the epoxidation reactions of alkenes, showing similar results with the homogeneous catalyst system [15].

The mesoporous silica with the pore diameter of 4.0 nm showed the largest adsorption capacity for metalloporphyrins [16, 17]. The state of the art in silica-based mesoporous multifunctional nanoparticles is oriented to: controlled dimensions of pores, ordered pore network, high surface area [18]. Based on previous reports on hybrid silica materials immobilizing porphyrin derivatives [19, 20], this work is focused on *in situ* entrapping of 5,10,15,20-tetrakis(4-pyridyl)porphyrin-Zn(II), (ZnTPyP), by sol-gel technique, starting from tetraethylorthosilicate

* Corresponding author: efagadar@yahoo.com

(TEOS). The sol-gel process was conducted by acid or acid-base catalysis, followed by sonication. A comparison between the properties of the obtained hybrids as a consequence of the used catalytic system and of supplementary treatments is done.

2. Experimental

The synthesis and some photophysical characteristics of ZnTPyP and of the porphyrin base were previously reported [21, 22]. Tetraethoxysilane (TEOS, ≥99%, Fluka) tetrahydrofuran (98% THF) and ethanol (99.2%, EtOH) from Merck, hydrochloric acid (37% HCl) and ammonia solution (25% NH_3) from Silal Trading and distilled water were all used without further purification.

Sol-gel preparations were started from tetraethoxysilane, absolute ethanol, distilled water, hydrochloric acid. The following mole ratios: TEOS:EtOH:H_2O:HCl=1:4:4:0.01 were kept constant during the first acidic step. Mole ratio of ZnTPyP:TEOS in all hybrid samples was $0.08*10^{-3}$:1.

In situ synthesis (conditions given in Table 1). Acid catalyzed method: a mixture of distilled water (4.50 g, 0.25 mol), EtOH (10.37 g, 0.225 mol) and HCl (0.0613 g, 0.000622 mol) was added by slow dropping under vigorous stirring to a solution of TEOS precursor (13.02 g, 0.0625 mol) dissolved into absolute EtOH (1.15 g, 0.025 mol). ZnTPyP (0.0037 g, 0.005 mmol) was dissolved into 20 mL THF and after 60 minutes was added by once to the silica precursor solution. The sol was kept at room temperature until gelation (60 days). *Two steps acid/base catalyzed method*: after the acid step, previously described, the second basic step consisted in slowly dropping of 2.5% NH_3 solution, until instantly achieved the gelation point. *Sonocatalysed method:* the mixture obtained in acid catalyzed process was ultrasonically treated. The parameters of sonication were: the pulses number-180, amplitude-20%, pulse on -15 s and pulse off - 5 s. The total amount of applied energy was 13800 J. The final gels were washed by distilled water. No leaching was observed. The same procedure was used to synthesize *control silica matrices*, without addition of ZnTPyP.

Table 1. Conditions of sol-gel synthesis and some textural characteristics and thermal analysis data.

No	Description of samples	Cat.*	Cat./ TEOS (mole ratio)	Textural characterization				Weight loss (%)			
				D_p [ads] (nm)	D_p [des] (nm)	S_{BET} (m^2/g)	V_p (cc/g)	25-200 ˚C	200-350 ˚C	350-600 ˚C	Total
(1)	Control sample - acid catalyzed	HCl	0.01/1	3.65	3.07	703.3	0.462	21.7	1.57	3.93	26
(2)	Hybrid sample - acid catalyzed	HCl	0.01/1	3.62	3.02	469.7	0.245	16.1	1.79	3.01	20.1
(3)	Control sample - acid-base catalyzed	HCl NH_3	0.01/1 0.015/ 1	3.40	3.81	1074.5	0.792	34	1.1	3.35	36.9
(4)	Hybrid sample - acid-base catalyzed	HCl NH_3	0.01/1 0.015/ 1	3.40	3.44	729.3	0.409	23.3	1.44	2.59	26.4
(5)	Control sample - acid and sono-catalyzed	HCl US**	0.01/1	3.08	3.08	432.1	0.226	15.1	1.82	3.05	19.2
(6)	Hybrid sample - acid and sono-catalyzed	HCl US**	0.01/1	1.97	1.97	347.1	0.134	16.8	1.66	2.94	20.6

*Cat. = catalyst ** US=ultrasonic field

The ultrasonic treatment was carried out by using a Sonics Vibra-Cell high intensity ultrasonic processor, 750 Watt VCX Model. FT-IR spectra were performed on JASCO 430 spectrophotometer as KBr pellets. Thermal analysis was done with a TGA/SDTA 851-LF Mettler-Toledo apparatus. UV-visible spectra were recorded on a JASCO V-650 model. The luminescence spectra were obtained on a Perkin Elmer LS55 by using accessory for powders. A 515 nm cut-off filter to eliminate harmonic or scattering peaks was used. Emission spectra were obtained using as excitation wavelength the Soret band. The N_2 adsorption–desorption isotherms are obtained on a NOVA 1200e at 77 K. The surface area (S_{BET}), the pore volume (V_P) and the pore diameter (d_P) are calculated by BET and BJH methods (Table 1). Atomic force microscopy (AFM) investigations, in contact or tapping mode, were performed with a Nanosurf® EasyScan 2 Advanced Research AFM. Samples were obtained onto a pure silica plate by slow evaporation of the solvent from a solution of the hybrids in THF [23].

3. Results and discussion

The FT-IR spectra of all samples display intense absorption peaks associated to the SiO_2 phase around 460, 800, 950, 1080 and 1180 cm^{-1}. They have been assigned to the Si-O-Si vibration bending modes, Si-O-Si symmetric stretching, Si-OH group, transversal (TO) and longitudinal optic (LO) Si-O-Si asymmetric stretching. The bands around 1065 cm^{-1} and 1105 cm^{-1} corresponds to the Si-O-C asymmetric stretching mode in ring/open link. The band at 1620 cm^{-1} is assigned to adsorbed molecular water. The broad absorption band between 3000 and 3800 cm^{-1} corresponds to stretching vibrations of hydroxyl groups [24, 25]. The FT-IR spectrum of ZnTPyP displays the main bands at 992 cm^{-1}, attributed to bending vibrations of C-N, an intense band at 1593 cm^{-1} due to stretching vibration of C=C in the pyridyl aromatic ring and another band at 793 cm^{-1}, attributed to the vibration of C-H bond from pyrrole. In the spectra of hybrids the characteristic bands of ZnTPyP groups were not clearly identifiable because they overlap with the broad bands of Si-O-Si and Si-O-C in hybrid material [26]. From the point of view of electronic spectra zinc-porphyrins represent the group of *normal* porphyrins [27], with an intense Soret band at 422 nm and only two Q bands of smaller intensity, in which the electronic transition Q(0,1) is more intense than Q(0,0). The electronic configuration of zinc atom is d^{10} and the interactions between the porphyrin π-system and the metal are somewhat small [28].

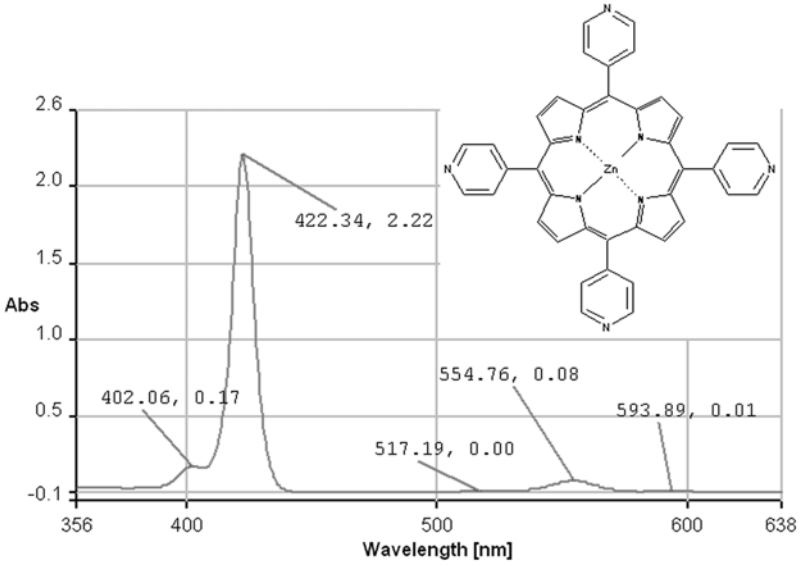

Fig. 1. The UV-vis spectrum in THF and the structure of ZnTPyP

The UV-vis spectrum of hybrid material obtained in two steps acid-base catalysis (Figure 2- curve 4) presents the Soret band and the Q bands almost in the same position with bare Zn-porphyrin. In comparison, the UV-vis spectra of hybrid materials obtained in acid catalysis, with or without ultrasonic treatment (Figure 2- curves 2 and 6), display large bathochromically and hyperchromically shifted Soret band around 450 nm and two Q bands also manifesting these effects, near 594 and 645 nm. These materials can be considered wide band absorbing materials with potential application as harvesting antenna for photovoltaic devices.

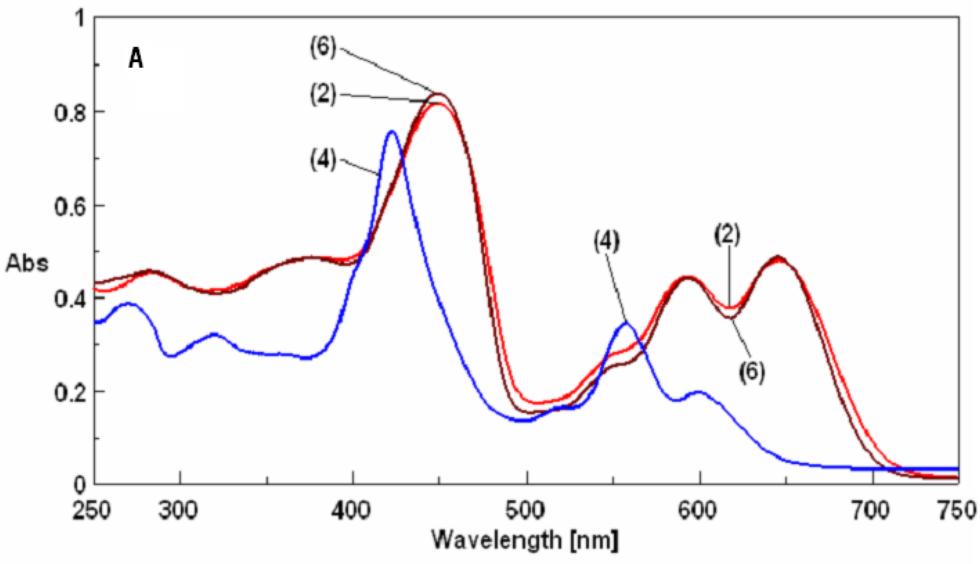

Fig. 2. Overlapped UV-vis spectra of (2), (6) and (4) hybrid samples, as powders. Curve labels correspond to the samples numbering from Table 1.

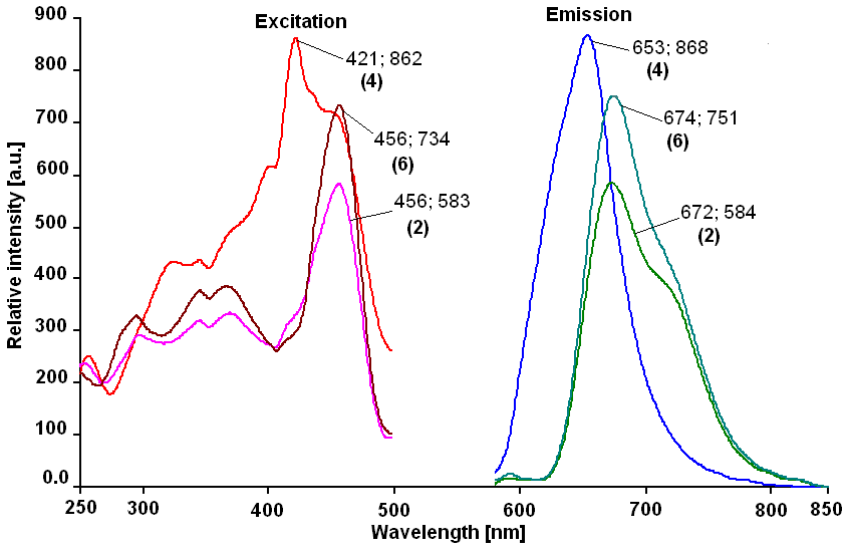

Fig. 3. Overlapped excitation and emission spectra of (2), (6) and (4) hybrid samples, as powders. Curve labels correspond to the samples numbering from Table 1.

A comparison of the previously reported emission spectra of porphyrin base, 5,10,15,20-tetra(4-pyridyl)-21H,23H-porphine (TPyP), registered in THF [21], and of (TPyP)-silica hybrid materials obtained by using acid catalysis [20], exhibit two emission bands around 650 and 710 nm (upon excitation at 395 nm), and at 655 nm and 715 nm, (by excitation at 420 nm), respectively. An exception is occurring regarding the Zn-metallated complex, which exhibits two emission maxima around 600 and 660 nm by excitation at 395 nm. The 600 nm band is characteristic of the metallated complex [21].

The Zn-metallated complex hybrid materials reveal very interesting changes regarding the position and the intensity of the emission bands, depending of the type of sol-gel catalysis and of the ultrasonically treatment. Therefore, in case of hybrids obtained by two steps acid-base catalysis (Figure 3- curve 4), the position of maximum is situated around 655 nm. For the one step acid catalyzed sample (Figure 3- curve 2) the emission is less intense and bathochromically shifted with almost 20 nm. In case of hybrid acid catalyzed ultrasonically treated sample (Figure 3- curve 6), the emission intensity is more intense, but does not reach the intensity of the two steps catalyzed sample. As for the sample without ultrasonic treatment, this increase is accompanied by the same bathochromic shift of 20 nm. In case of acid catalysis the emission bands are wide, from 620 nm to 820 nm, in the red domain, which is important in case of medical use for photodynamic therapy of cancer.

Thermal and textural analysis of the novel nanomaterials are presented in Table 1. The weight loss profiles of all the silica xerogels are quite similar, and their thermal decompositions performed in the programmed temperature range of 25–600 °C occur through three-steps process. Every silica system shows an endothermic peak at 80 °C due to the elimination of physically adsorbed water, corresponding to 15-34 % weight loss evidenced by the thermogravimetric analysis. The exothermic peak around 430 °C corresponds to the combustion of organics. The weight lost accompanying that peak is about 3-4 %.

The N_2 isotherms show type IV character, specific to mesoporous systems, with a H3 hysteresis loop, indicating the presence of slit-shape pores. The dimension of the pores is narrowly distributed in the range of 2-3.8 nm. Every introduction of Zn-porphyrin in the silica gels produced the decrease in the surface area in comparison with the control samples. This is a certain proof that the porphyrin is trapped inside the silica network. The highest surface area was obtained in case of acid base catalysis and the lowest (almost half) in case of acid catalysis followed by sonosynthesis, due to reorganizing of nanomaterial structure.

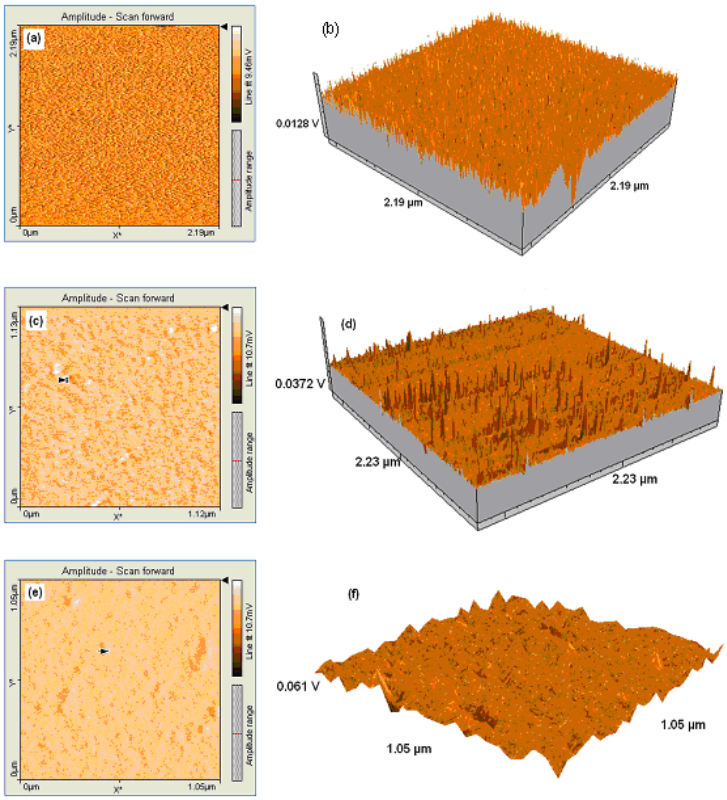

Fig. 4. 2D and 3D (NanoSurf EasyScan2) images of ZnTPyP-hybrid materials: sample 2-(a) and (b); sample 4-(c) and (d); sample 6-(e) and (f). Curve labels correspond to the samples numbered in Table 1.

The 2D and 3D AFM images show for hybrids obtained by two steps acid-base catalysis (Figure 4-c and d), columnar stacks of 52.2 nm both in length and in width. The dimension of the particles is a little smaller in hybrids obtained by acid catalysis (Figure 4-a and b) of only 48.2 nm in diameter, but in case of further treatment with ultrasonic field (Figure 4-e and f) the particles are reorganized growing to pyramids having base dimensions of 65.6 nm. The height of the aggregates is around 4-6 nm, in all the hybrids.

4. Conclusions

Entrapping of **ZnTPyP** by sol-gel technique was conducted by acid or acid-base catalysis, followed by sonication. Nanomaterials with high surface area (350-730 m^2/g), narrowly distributed pore size (2-3.8 nm), exhibiting intensive absorption of light in the red-region up to 700-800 nm were obtained. The nanomaterials obtained by acid catalysis are exhibiting both in electronic and emission spectra bathochromic shifted bands in comparison with the hybrids obtained in two steps catalysis; supplementary, in emission spectra of sonocatalyzed samples hyperchromic effects are noticed. AFM images show for hybrids obtained by non-sonicated samples columnar stacks around 50 nm in diameter. In case of further treatment with ultrasonic field the particles are reorganized growing to pyramids of increased dimensions.

Acknowledgement

Authors wish to thank Romanian PNII-D11-055 for granting.

References

[1] D. Chen, D. Yang, J. Geng, J. Zhu, Z. Jiang, Appl. Surf. Sci. **255**, 2879 (2008).
[2] G. Mihailescu, L. Olenic, S. Pruneanu, E. Fagadar-Cosma, P. Ardelean, E. Indrea, S. Dreve, T. D. Silipas, J. Optoelectron. Adv. M. **10**, 2252 (2008).
[3] S. M. S. Chauhan, P. Kumari, Tetrahedron **65**, 2518 (2009).
[4] P. Bhyrappa, V. Velkannan, Tetrahedron Lett. **51**, 40 (2009).
[5] G. Fagadar-Cosma, D. Vlascici, E. Fagadar-Cosma, J. Biol. Inorg. Chem. **12**, 218 (2007).
[6] J. Matsui, T. Sodeyama, Y. Saiki, T. Miyazawa, T. Yamada, K. Tamaki, T. Murashima, Biosen. Bioelectron. **25**, 635 (2009).
[7] Y. Q. Weng, Y. L. Teng, F. Yue, Y. R. Zhong, B. H. Ye, Inorg. Chem. Commun. **10**, 443 (2007).
[8] R. Cristescu, C. Popescu, A. C. Popescu, I. N. Mihailescu, A. A. Ciucu, A. Andronie, S. Iordache, I. Stamatin, E. Fagadar-Cosma, D. B. Chrisey, Mater. Sci. Eng. B-Adv. **169**, 106 (2010).
[9] J. Matsumoto, T. Matsumoto, Y. Senda, T. Shiragami, M. Yasuda, J. Photoch. Photobio. A **197**, 101 (2008).
[10] G. Mihailescu, L. Olenic, S. Garabagiu, G. Blanita, E. Fagadar-Cosma, A. S. Biris, J. Nanosci. Nanotechno. **10**, 2527 (2010).
[11] D. K. Deda, A. F. Uchoa, E. Carita, M. S. Baptista, H. E. Toma, K. Araki, Int. J. Pharm. **376**, 76 (2009).
[12] C. Ringot, V. Sol, R. Granet, P. Krausz, Mater. Lett. **63**, 1889 (2009).
[13] Z. Deyl, I. Miksik, A. Eckhardt, V. Kasicka, V. Král, Curr. Anal. Chem. **1**, 103 (2005).
[14] J. S. Hu, Y. G. Guo, H. P. Liang, L. J. Wan, L. Jiang, J. Am. Chem. Soc. **127**, 17090 (2005).
[15] A. R. McDonald, N. Franssen, G. P. M. van Klink, G. van Koten, J. Organomet. Chem. **694**, 2153 (2009).
[16] H. Akasaka, H. Yukutake, Y. Nagata, T. Funabiki, T. Mizutani, H. Takagi, Y. Fukushima, L. R. Juneja, H. Nanbu, K. Kitahata, Micropor. Mesopor. Mat. **120**, 331 (2009).
[17] E. Fagadar-Cosma, M. C. Mirica, I. Balcu, C. Bucovicean, C. Cretu, I. Armeanu, G. Fagadar-Cosma, Molecules **14**, 1370 (2009).

[18] H. J. Kim, K. J. Shin, M. K. Han, K. An, J. K. Lee, I. Honma, H. Kim., Scripta Mater. **61**, 1137 (2009).
[19] E. Fagadar-Cosma, C. Enache, D. Vlascici, G. Fagadar-Cosma, M. Vasile, G. Bazylak, Mater. Res. Bull. **44**, 2186 (2009).
[20] E. Fagadar-Cosma, C. Enache, D. Dascalu, G. Fagadar-Cosma, R. Gavrila, Optoelectron. Adv. Mat. **2**, 437 (2008).
[21] E. Fagadar-Cosma, C. Enache, I. Armeanu, G. Fagadar-Cosma, Dig. J. Nanomater. Bios. **2**, 175 (2007).
[22] E. B. Fleischer, E. I. Choi, P. Hambright, A. Stone, Inorg. Chem. **3**, 1284 (1964).
[23] E. Fagadar-Cosma, C. Enache, I. Armeanu, D. Dascalu, G. Fagadar-Cosma, M. Vasile, I. Grozescu, Mater. Res. Bull. **44**, 426 (2009).
[24] C. J. Brinker, G.W. Scherer, Sol-Gel Science: The Physics and Chemistry of Sol-Gel Processing, Academic Press Inc., New York (1990).
[25] R. Al-Oweini, H. El-Rassy, J. Mol. Struct. **919**, 140 (2009).
[26] H. Kaddami, J. F. Gerard, P. Hajji, J. P. Pascault, J. Appl. Polym. Sci. **73**, 2701 (1999).
[27] T. N. Lomova, B. D. Berezin, Russ. J. Coord. Chem. **27**, 85 (2001).
[28] M. Gouterman, In The Porphyrins, Vol. III, Ed. D. Dolphin, Academic Press, New York (1978).